

Force-Sensitive Prosthetic Hand with 3-axis Magnetic Force Sensors

Ann Marie Votta

Soft Robotics Laboratory
Worcester Polytechnic Institute
Worcester, Massachusetts
amvotta@wpi.edu

Sezen Yağmur Günay

Cognitive Systems Laboratory
Northeastern University
Boston, Massachusetts
gunay@ece.neu.edu

Deniz Erdoğan

Cognitive Systems Laboratory
Northeastern University
Boston, Massachusetts
erdogmus@ece.neu.edu

Çağdaş Önal

Soft Robotics Laboratory
Worcester Polytechnic Institute
Worcester, Massachusetts
cdonal@wpi.edu

Abstract—In this paper, we investigate the use of 3-dimensional force sensors in a prosthetic hand. 3-dimensional force sensing in prosthetics can be used to incorporate intelligent grasping capabilities, allowing the hand to automatically adjust its grasp or release an object when appropriate. This can significantly decrease the burden on the user as well as increase the functionality of the prosthetic. Coupled with an underactuated hand, this opens up possibilities for highly functional, affordable prosthetic hands. In this work, we present our design of 3D magnetic force sensors that are embedded within the fingers of an open-source, 3D printable underactuated hand. We implement a simple control scheme using both shear and normal force readings to automate grasp release. Finally, we combine this force control with EMG grasp detection for a series of pick-and-place tasks. Preliminary results suggest that intelligent grasp control imposes less of a burden on the user than a completely EMG-based grasp control.

Index Terms—Force sensing, smart prosthetic, intelligent grasping

I. INTRODUCTION

Despite significant advances in state-of-the-art hand prostheses, there remains a distinct trade-off between functionality and affordability for actuated hands. The high cost of prostheses is largely driven by the need for extremely precise actuation and sensing and complex control. This level of precision is needed for rigidly actuated hands, which describes the majority of commercial prostheses.

Underactuated hands, such as those in [1], [2], and [3], are becoming increasingly appealing to researchers as a way to decrease the complexity and cost of a hand. While rigid hands require high degrees of actuation and precise position control to facilitate multiple grasp types and grasp a variety of objects, underactuated hands have the advantage of being able to adaptively conform to whatever object is being grasped.

Neuromuscular driven upper-limb prostheses have also been the focus of an increasing number of researchers due to their potential for easing the lives of millions worldwide. The higher signal-to-noise ratio of the surface electromyogram (EMG) signals is considered one of the most appealing pathway to convey user's intentions to the prosthetic limb. In most applications, simple open and close EMG commands are

given by a user, who has to manually select a grasp type. In [4], Günay et. al. represent all useful muscle patterns as combinations of a small number of generators, and in doing so can detect multiple grasp types from a user. A potential problem with this approach, depending on the implementation, is that the user must maintain the desired grasp type to keep the prosthetic hand in the desired pose. This can place unnecessary burden on the amputee when grasping objects for extended periods of time.

One way to alleviate this burden is by incorporating force sensors to enable intelligent grasping capabilities. Normal force in prosthetic hands (Figure 2a, blue arrow) is extremely useful as it allows the control of grasp force, which is crucial to a stable grasp. Shear force (Figure 2a, orange and yellow arrows) is also crucial to grasp stability, and having sensors that measure shear force can enable more complex functionalities, such as identifying when an object is lifted or if it slips. This can in turn help reduce the burden on the amputee, who now does not need to actively think about maintaining their grasp on an object.

In this work, we present a 3D magnetic force sensor embedded in an open-source, affordable advanced prosthetic. Our 3D printable hand, built off Open Bionics' open-source Ada hand [5], is underactuated to allow for compliant grasping. It additionally is equipped with embedded custom 3-axis force sensors, enabling force control with the hand using shear and normal forces. To capture user intent, we use the Myo Armband to acquire EMG data and employ an Extremely Randomized Tree (Extra-Tree [6]) Classifier to predict the user's grasp type.

II. PREVIOUS WORK

Force sensors that detect contact forces are the most commonly used for grasping applications. Force sensitive resistors (FSRs) are commonly used to control the grasp force of a hand on an object [7], [8]. In [9], Koiva et al. create a 3-dimensional sensor composed of multiple FSRs on a curved surface, which is form fit to the fingertip. This sensor can measure the normal force at multiple contact points around the fingertip, enabling them to pinpoint more precisely where contact forces are applied. This type of contact-force control is extremely useful, as it can be used to prevent excessive deformation of grasped

Our work is supported by National Science Foundation (NSF) (CNS-1544636, CPS-1544895, CPS-1544636, CPS-1544815) and National Institutes of Health (NIH) (R01DC009834).

objects, but cannot provide information about shear forces or object slip. Some works have explored using FSRs for slip prevention in addition to traditional grasp force control [10], [11], but these methods require extensive signal processing to obtain a slip signal from an FSR, and additionally still lack the ability to read shear forces directly.

Less commonly used sensors in prosthetic grasping applications are those that measure shear force. In [12], the authors develop a fingerpad-like sensor that uses 2 strain sensors to measure shear force. The sensor works much like a human fingerpad- when a shear force is applied to a microfluidic skin, the skin is deformed in the direction of applied shear, causing tension in one strain sensor and compression in the other. In [13], authors present an optical based sensor that can measure shear force in 2 axes. Authors in [14] use multiple strain gages on a single finger to detect shear force at multiple locations on the finger, and perform proportional, proportional-derivative, and slip-prevention control on a robotic gripper. These sensors, unlike contact force sensors, can provide useful information about slip and shear force without too much complexity. However they cannot measure normal forces, which limits their ability to be used for grasp force control.

Numerous examples of sensors combining shear and normal force readings exist in the literature. Sensors described in [15] and [16] use optical-based sensing to measure shear and normal forces. In [17], authors map a change in capacitance, either from decreased distance or decreased area between two plates, to a 3 dimensional force. Similarly in [18], authors present promising results using a capacitive sensor to measure shear and normal forces on human fingers during object grasping. Authors in [19] present a magnetic force sensor that uses a 3-axis hall effect sensor and magnet to measure 3 dimensional forces. These sensors, as well as the majority of other force sensors, have one major flaw. The biggest shortcoming for many sensors is that they have a very small contact area for which they can measure forces. They may work well if the finger contacts an object on the exact location of the sensor, but if contact occurs anywhere outside the sensor, the sensor cannot read any forces.

Few researchers have addressed this problem, and as a result almost all existing force sensors meant for prosthetic hands have a small contact area. In [20], Nasir et al. embed two small load cells in the tip of each finger on a 3-fingered robotic gripper. Because the load cells are embedded in the structure of the finger, the sensor is less limited in location of applied force compared to many other sensors. However, the load cells can only measure compressive forces, so these fingers only measure force in 2 directions- normal force applied to the front of the fingertip and normal force applied to the top of the fingertip. In [21], Park et al. develop hollow, cylindrical robotic fingers with Fiber Bragg Grating sensors embedded within the finger structure. Each finger, using 4 FBG strain sensors, can measure longitudinal location (length along finger), latitudinal (circumferential) location, and magnitude of an applied force. These sensors, while quite effective, require highly specific equipment to obtain meaningful data from

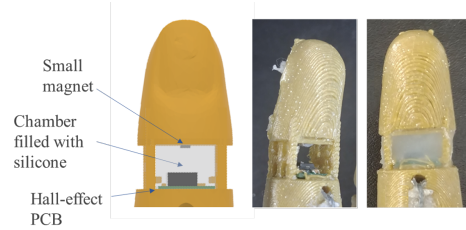


Fig. 1. Embedded hall-effect sensor. As the fingertip is deflected relative to the rest of the finger, the magnet moves relative to the hall-effect sensor, causing a change in magnetic field.

raw sensor signals, and are relatively expensive. Signals from our sensors are directly related to force, so meaningful force data can be obtained in real time from most microprocessors. Finally, the SynTouch BioTac sensors have been incorporated into numerous state-of-the-art systems ([22], [23]), due to their impressive ability to detect 3D forces, vibrations, and temperature. However their cost of about \$15,000 per sensor makes them incredibly impractical for any application where low cost is desired.

We present an affordable novel force sensor that measures 3-dimensional forces applied anywhere on the fingertip. To the best of our knowledge, no other 3D force sensor like this exists that is embedded within the finger itself. Furthermore, the sensors are extremely affordable (about \$6 per sensor), and can be used to implement intelligent grasping capabilities in the hand to decrease the burden on the user.

In the remainder of the paper, we present the force sensor design, a real-time EMG classification framework (Section II), the grasping experiments performed using the sensors (Section III), and conclusions and future work (Section IV).

III. MATERIALS AND METHODS

A. Force Sensor Design

Our force sensor is based on the magnetic sensing technology presented in [19], and is embedded within the finger link itself. The sensors are embedded in the Open Bionics Ada Hand, which we modified to fit our needs. The Ada Hand is a 5-fingered anthropomorphic underactuated hand, with five linear actuators driving 5 tendons, one for each finger. The entire hand is 3D printed out of Ninjabflex, a flexible filament.

Figure 1a shows the final design of the sensor and fingertip. Each finger has a rectangular cavity, with grid-like side walls, also 3D printed from Ninjabflex, to keep the finger together and guide the deformation of the fingertip. At the bottom of the cavity, attached to the bottom portion of the finger, is a PCB with a 3-axis hall-effect sensor. At the top of the cavity, attached to the top portion of the finger, is a small magnet. The cavity itself is filled with silicone (Ecoflex 00-30) to hold the PCB and magnet in place, as well as to add stiffness and prevent excessive deformation of the fingertip. Figures 1b and 1c show the built sensor without and with silicone.

During grasping, if a finger makes contact with an object anywhere on the fingertip above the sensor, the top of the fingertip is deformed in some direction relative to the bottom of

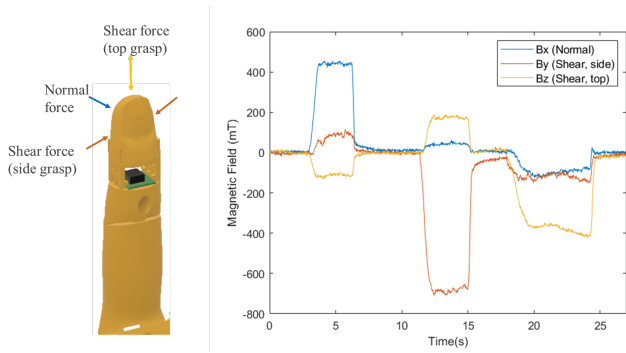


Fig. 2. The embedded sensor can read changes in force in 3 dimensions. An applied normal force results in a change in B_x , shear force caused by a side grasp changes B_y , and shear force caused by a top grasp changes B_z .

the finger, moving the magnet relative to the hall-effect sensor. This results in a shear or normal force reading, depending on the direction of applied force. Figure 2 shows the raw x-y-z magnetic field readings from as sensor when pushed first in the positive x (normal) direction, then the negative y (shear during a side grasp), and finally negative z (shear during a top grasp). When the fingertip is pushed in a given direction, the magnetic field on that axis changes the most significantly. The other two axes also change, although much less so, as it is almost impossible to move the fingertip in one direction without it also deforming slightly in the others.

B. Force Sensor Calibration

Each fingertip force sensor was calibrated using a load cell. For each finger, force sensor and load cell data were recorded as the fingertip was pushed against the load cell in the positive normal direction and in the positive and negative shear directions. This data provided a calibration constant for each finger and each direction that would relate the force sensor reading with an actual force, in grams. Because the sensor is more directly measuring deflection than actual force, the sensor reading for a given force depends on where along the fingertip the force is applied.

Figure 3 shows the x and y magnetic field readings of the thumb sensor when a 150g weight is hung from it, applying a force in the normal direction. On the left side of the graph the weight is hung as close to the sensor as possible, whereas on the right side it is hung closest to the end of the thumb. The moment and hence the displacement is larger the farther the force is applied from the sensor, so there is a larger reading on the right side of the graph than on the left side, for the same applied force. For our calibration, we used the center of each fingertip as consistently as possible for each push against the load cell. However we recognize that this calibration is not perfect, and that forces obtained during grasping experiments inherently contain some error.

Figure 4a shows a sample data set before and after calibration. In this case, a force was applied in the positive shear direction of the thumb. To achieve this, the side of the thumb was pushed against the load cell 5 times. The top graph shows

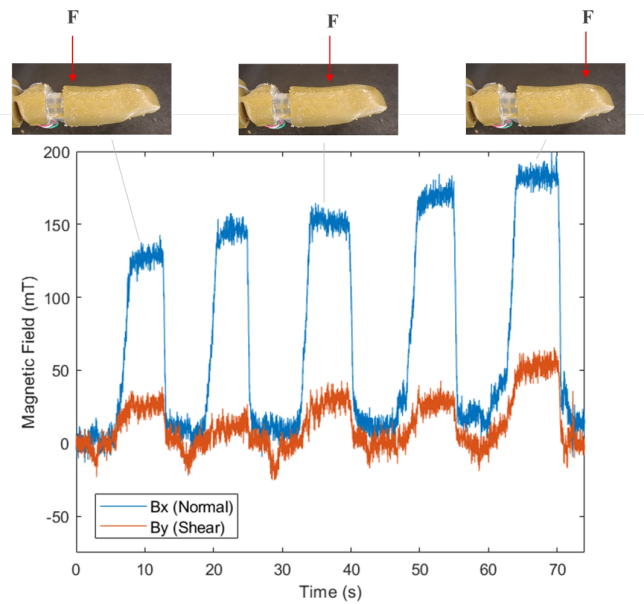


Fig. 3. Depending on the location of the applied force, the sensor reading changes. For a constant applied force of 150g (1.47N) in the normal direction, the raw B_x reading varies from 140mT when applied closest to the sensor, to 175mT when applied closest to the tip.

that the normal force stays close to zero throughout the test, and the shear force and load cell seem to change proportionally to each other but with different magnitudes. A constant was calculated for each peak in the load cell and force sensor data, and a single calibration constant taken as the average of these. For this set of data the calibration constant is 0.873, and once this is applied to the shear force it very closely matches the load cell reading (Figure 4b).

C. EMG Acquisition and Real-Time Classification

EMG classification used in this work can be grouped in two categories: calibration and real-time testing. To calibrate the EMG classifier, surface EMG data sampled at 50 Hz was recorded for 5 sessions from 8 channels. Each session consists of a 5 second recording for each class. The subject was asked to perform a particular gesture and maintain the gesture until the trial time was over. After the recording was completed, the protocol was repeated for another gesture, and again until calibration data was collected for each gestures 5 times. Since the recorded gesture labels were known during data acquisition, the labels and EMG time samples were fed to an Extra-Tree classifier for training an offline model. The model was trained in Python using the scikit-learn library (number of trees was assigned as 10, the nodes were expanded until all leaves were pure or until all leaves contained less than 2 samples). The trained model was conveyed to the real-time classification framework where the test EMG data was sampled at the same frequency. The buffer length was selected as 20 samples and the confidence threshold as 80%. After the first 20 samples, the classification was run and if the threshold confidence was exceeded the gesture label was sent to the

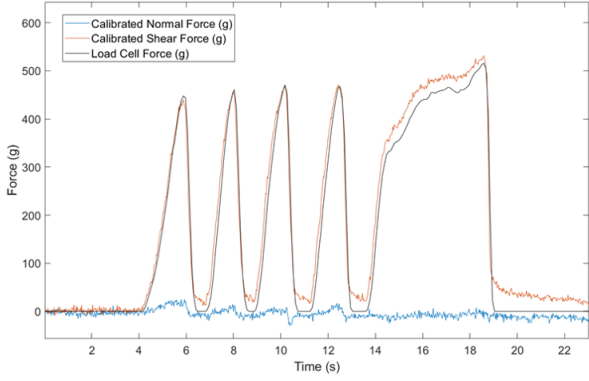
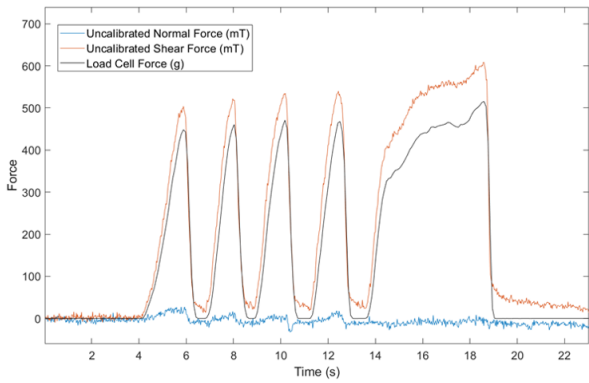


Fig. 4. Normal and shear force readings before (in mT) and after (in g) calibration with a load cell. This graph shows the calibration results from an applied shear force on the thumb.

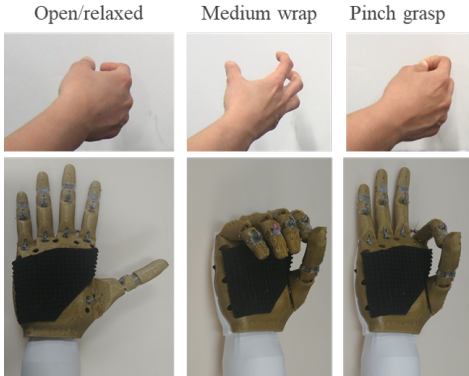


Fig. 5. With EMG, a user can select between open, medium wrap, and pinch grasp types for the robotic hand.

prosthesis. However, if the model confidence was not satisfied after the buffer size, a new sample was collected by employing a stock data structure until the threshold was satisfied.

IV. EXPERIMENTAL RESULTS

A. Force Control with Automatic Release

Using these sensors, we implemented simple force control using normal and shear forces. The controller is designed for pick-and-place tasks, to realize and maintain a stable grasp on an object and automatically release it when the user places the

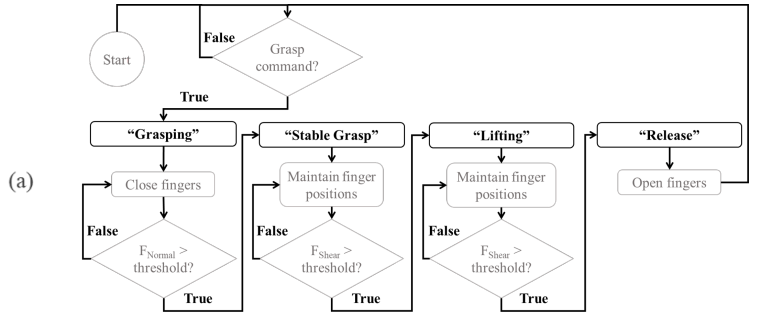


Fig. 6. State machine diagram of simple normal and shear force control of a hand.

object on a table. For simplicity, we chose to focus on lifting using side grasps, so we only used the y-direction shear force and neglected the z-direction shear force that changes during a top grasp lift. The control scheme, shown in Figure 6 has four states: Grasping, Stable Grasp, Lifting, and Release.

First, a grasp command is sent by the user, which can be either a medium wrap or pinch. Once this command is sent, the hand enters the “Grasping” state, at which point it closes its fingers until the normal force reaches an experimentally determined normal threshold. Once this normal threshold is reached, the hand has a stable grasp on the object, and it enters the “Stable Grasp” state. Here it begins monitoring the shear force in the fingers. If the shear force is below some shear threshold, the hand remains in the stable grasp state, but if it increases above the shear threshold, the hand is lifting an object and it enters the “Lifting” state. Here it continues to monitor the shear force. If the shear force stays above the shear threshold value, the hand stays in the lifting state, and if it drops below the shear threshold the object has been placed back on the table (or someone’s hand), so it switches to the “Release” state, at which point it opens the fingers to release the object.

B. Preliminary User Test with EMG

To validate the usefulness of the automatic-release force control, we performed a series of pick-and-place tasks using the automatic release. For these experiments, a single experienced user selected either a medium wrap or pinch grasp for the hand using EMG. The user assumed a hand posture corresponding to the desired grasp type, maintained this posture for 1-2 seconds, then relaxed her hand as the robotic hand took control of grasping. A second person held the robotic hand in position to grasp, lifted it once it had grasped the object, and placed it back down a predetermined distance away from the object’s starting location. We performed pick-and-place for 9 objects; 5 were grasped using both grasp types, and 2 objects each were grasped using just a medium wrap and just a pinch grasp. Each grasp was repeated until it has been successfully completed 4 times, so a total of 14 successful grasps were completed for each grasp type per trial. This entire experiment was repeated without automatic grasp release, where the user maintained hand posture for the selected grasp type for the

entire pick-and-place task and relaxed her hand at the end to release the object. A link to a video of the task can be found in Section VI Additional Materials. Figure 7a shows a grasping sequence during an experiment with the automatic grasp release, while Figure 7b shows a grasp sequence without. In the top image, the user’s hand is relaxed for the majority of the pick-and-place task, while in the bottom image her hand is tense for the entire task, until she relaxes it to send a “release” signal to the robotic hand.

Figures 8 and 9 show the shear and normal force readings, motor inputs, grasp state, and EMG state during two pick-and-place tasks. The EMG state (dashed black line) is at 200 for a medium wrap and 400 for a pinch grasp. The grasp state (solid black line) is 0 for “Open” or “Release,” 200 for “grasping,” 300 for “Stable Grasp,” and 400 for “Lifting.” A motor value of 0 corresponds to the finger being fully open, and 950 corresponds to completely closed.

Figure 8 shows a pinch grasp pick-and-place task using the automatic release feature. Initially the fingers are all open. After an EMG grasp command is sent, the grasp state changes from “Open” to “Grasping,” at which point the fingers begin to close. They close until the normal force threshold is reached for both the thumb and index finger (in this case about 30g and 70g respectively), then maintain their position. The state changes to “Grasping,” and the shear and normal forces remain mostly constant while the hand maintains its current pose. Now the hand monitors the shear forces, and when they significantly change, the grasp state changes to “Lifting.” Again, the hand maintains its pose, and once the object is in the air the shear and normal forces remain fairly constant. Finally, the object is placed on the table, which is recognized by another large change in shear force, at which point the grasp state changes to “Open,” the fingers open, and the forces go back to zero.

Similarly, Figure 9 shows a medium wrap pick-and-place task without automatic grasp release. Here there is one fewer grasp state (no “Lifting” state), and the EMG state remains a medium wrap for the duration of the task. The force profiles are similar to those in Figure 8a, with the addition of the middle finger forces. A noticeable difference between the graphs in Figures 8 and 9 is the amount of time between object placement and release. With the automatic release enabled, this transition is almost immediate, but without it there are multiple delays introduced. There is almost a full second between when the object is placed and the user relaxes her hand to release the object. Then the EMG classifier recognizes the relaxed/open state for a short time before mistakenly registering a pinch grasp, and then sending a final release command and opening the fingers.

For these experiments, a total of 56 pick-and-place tasks were successfully performed for each grasp type. Half of these were using automatic grasp release and half used EMG signals to command the hand to open. The entire experiment was performed by a single user who had considerable experience with the EMG system. While using the automatic release, objects were dropped mid-task more often than with EMG-release, especially for a medium wrap grasp type. We suspect

TABLE I
PICK-AND-PLACE RESULTS COMPARISON FOR AUTO-RELEASE AND EMG RELEASE CONDITIONS

	Auto-release	EMG release
Number of Trials	70	63
Med. Wrap Trials	39	30
Pinch Trials	31	33
Drops Med. Wrap	3	0
Drops Pinch	1	1
Failed Release Med. Wrap	3	2
Failed Release Pinch	3	4
Extended EMG Misclassification	13	25
Med. Wrap Success Rate	84.6%	93.3%
Pinch Success Rate	87.1%	84.8%
Overall Success Rate	85.7%	88.9%
EMG Classification Error Rate	18.6%	39.7%

the large number of drops is due to the grasping quality of the hand itself; due to its underactuated and compliant nature, the fingers can be easily shifted mid-grasp, causing changes in shear force that cause the hand to release an object too soon. On the other hand, the automatic release control had a slightly higher success rate in releasing objects upon placement than the EMG-release. When trying to release objects with EMG, there was sometimes a false grasp classification after the initial release, causing the hand to remain closed. We believe this is caused by muscle fatigue from maintaining an uncomfortable hand pose for extended periods of time during the EMG-release tasks. As the experiment progressed, the user became more tired and had more difficulty maintaining the the desired hand pose, which caused errors in the EMG classification. This was not a problem with automatic release, as the user was able to keep a relaxed hand for the entire task, after briefly choosing the grasp type.

We also found that there were significantly fewer EMG classifier errors in the trials with automatic grasp release than those with EMG grasp release. In the 70 trials using automatic grasp release, there were 13 trials where the EMG classifier was incorrect for a sustained time of greater than 0.25 seconds. By comparison, 25 out of 63 tasks performed using EMG release had a similar EMG classification error. This means that at any point in the task, the EMG grasp type was different from what the user intended for at least 0.25 seconds, which was enough time in some cases to cause the fingers to move undesirably. As with the failed releases, we believe this classification error stems from the user’s fatigue from maintaining a desired grasp during the EMG release tasks.

V. CONCLUSIONS AND FUTURE WORK

In this paper, we present the design and calibration of a 3D force sensor embedded in the finger itself. Unlike most existing sensors, its structure allows force to be measured in any direction no matter where it is applied on the fingertip, and is not limited to a small contact area. With the sensors embedded in an underactuated hand, we implemented a simple yet effective force control scheme using shear and normal forces to automate object release during pick-and-place tasks.

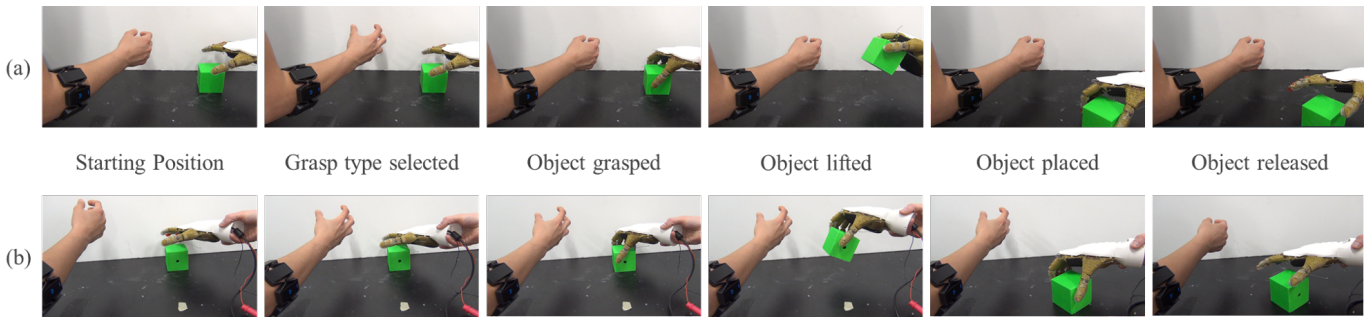


Fig. 7. Grasp sequence of a pick-and-place task. (a) Shear force is monitored to enable automatic release of the object, so the user can relax her hand for the majority of the task. The user's hand is tense only when initially selecting a grasp type (in this case Medium Wrap). (b) The user manually releases the object with EMG, thus the selected grasp type is maintained by the user through most of the task. The user's hand is tense during the majority of the task, potentially causing fatigue over time.

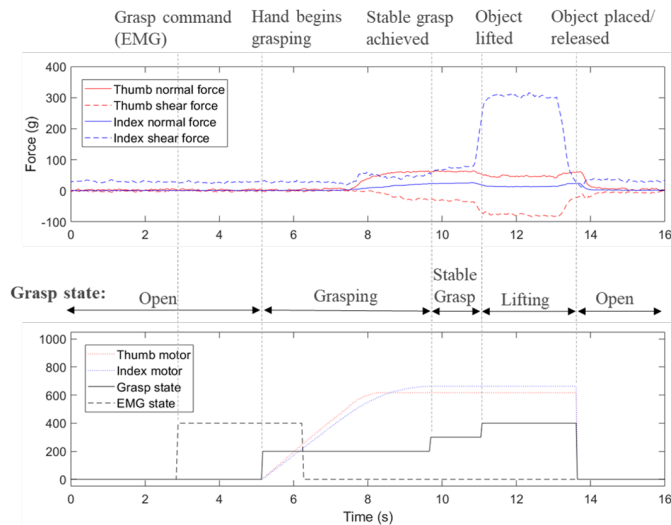


Fig. 8. Index and thumb forces and motor positions and EMG and Grasp states during a pick-and-place task with automatic grasp release enabled. The object is quickly released once it is placed on the table.

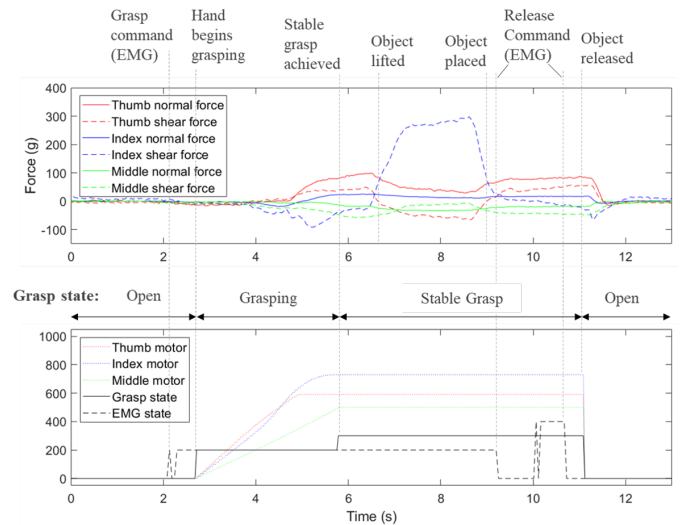


Fig. 9. Index, middle, thumb forces and motor positions and EMG and Grasp states during a pick-and-place task with automatic grasp release disabled. There is a significant delay between when the object is placed on the table, when the user sends the release command, and when the object is actually released.

Comparing this to experiments where the user manually released the object using EMG, we found slight improvements in reliability of object release, as well as a decreased burden on the user.

This preliminary work shows promising results for the use of these sensors in prosthetic applications and intelligent grasping. Our next steps are to incorporate the z-axis force reading to enable automatic release for top grasps and to further characterize the sensors. Currently, each sensor behaves differently due to manufacturing imperfections, and we hope to better standardize them, making them more consistent and easier to work with. Additionally there is some amount of drift present over time, as the fingertips often retain a very small amount deformation for some time after the force is removed. In the future we hope to eliminate this drift to make the sensors even more reliable. Besides the sensors, the hand itself presents problems due to its compliant nature and limited degrees of freedom. We would like to add slightly more rigidity to it to achieve more predictable behavior and more ideal force sensor

readings, as well as thumb opposition to achieve better grasp quality. Finally, we plan to complete more comprehensive user testing, with both experienced and inexperienced users, to explore whether the automatic grasping capabilities make the system more intuitive.

VI. ADDITIONAL MATERIALS

Below is a link to a video demonstration of our pick-and-place experiments:

<https://www.dropbox.com/s/z5ubcqve40xuiht/IEEEBionics2019Video.mp4?dl=0>

ACKNOWLEDGMENTS

Our work is supported by National Science Foundation (NSF) (CNS-1544636, CPS-1544895, CPS-1544636, CPS-1544815) and National Institutes of Health (NIH) (R01DC009834).

REFERENCES

- [1] Z. Teng, G. Xu, R. Liang, M. Li, S. Zhang, J. Chen, and C. Han, "Design of an underactuated prosthetic hand with flexible multi-joint fingers and eeg-based control," in *2018 IEEE International Conference on Cyborg and Bionic Systems (CBS)*. IEEE, 2018, pp. 647–651.
- [2] P. Khanna, K. Singh, K. M. Bhurchandi, and S. Chiddarwar, "Design analysis and development of low cost underactuated robotic hand," in *2016 IEEE International Conference on Robotics and Biomimetics (ROBIO)*. IEEE, 2016-12, pp. 2002,2007.
- [3] J. Zhao, L. Jiang, S. Shi, H. Cai, H. Liu, and G. Hirzinger, "A five-fingered underactuated prosthetic hand system," in *2006 International Conference on Mechatronics and Automation*, vol. 2006. IEEE, 2006-06, pp. 1453,1458.
- [4] S. Y. Günay, M. Yarossi, D. H. Brooks, E. Tunik, and D. Erdoğmuş, "Transfer learning using low-dimensional subspaces for emg-based classification of hand posture," in *2019 9th International IEEE/EMBS Conference on Neural Engineering (NER)*. IEEE, 2019, pp. 1097–1100.
- [5] "Ada v1.1 assembly instructions." [Online]. Available: <https://openbionicslabs.com/obtutorials/ada-v1-assembly>
- [6] P. Geurts, D. Ernst, and L. Wehenkel, "Extremely randomized trees," *Machine learning*, vol. 63, no. 1, pp. 3–42, 2006.
- [7] Q. Li and Y. Lv, "A fuzzy pid control method for the grasping force of an underactuated prosthetic hand," *Applied Mechanics and Materials*, vol. 551, no. Design, Manufacturing and Mechatronics, pp. 514,522, 2014-05-01. [Online]. Available: <http://search.proquest.com/docview/1541455158/>
- [8] T. Zhang, L. Jiang, and H. Liu, "A novel grasping force control strategy for multi-fingered prosthetic hand," *Journal of Central South University*, vol. 19, no. 6, pp. 1537–1542, 2012.
- [9] R. Koiva, M. Zenker, C. Schurmann, R. Haschke, and H. J. Ritter, "A highly sensitive 3d-shaped tactile sensor," in *2013 IEEE/ASME International Conference on Advanced Intelligent Mechatronics*. IEEE, 2013-07, pp. 1084,1089.
- [10] R. Barone, A. Ciancio, R. Romeo, A. Davalli, R. Sacchetti, E. Guglielmelli, and L. Zollo, "Multilevel control of an anthropomorphic prosthetic hand for grasp and slip prevention," *Advances in Mechanical Engineering*, vol. 8, no. 9, pp. 1,13, 2016-09-01. [Online]. Available: <http://search.proquest.com/docview/1826922676/>
- [11] H. Deng, G. Zhong, X. Li, and W. Nie, "Slippage and deformation preventive control of bionic prosthetic hands," *IEEE/ASME Transactions on Mechatronics*, vol. 22, no. 2, pp. 888,897, 2017-04.
- [12] J. Yin, P. Aspinall, V. J. Santos, and J. D. Posner, "Measuring dynamic shear force and vibration with a bioinspired tactile sensor skin," *IEEE Sensors Journal*, vol. 18, no. 9, pp. 3544,3553, 2018-05-01.
- [13] J. Missinne, E. Bosman, B. Van Hoe, R. Verplancke, G. Van Steenberge, S. Kalathimekkad, P. Van Daele, and J. Vanfleteren, "Two axis optoelectronic tactile shear stress sensor," *Sensors Actuators: A. Physical*, vol. 186, pp. 63,68, 2012-10.
- [14] E. Engeberg and S. Meek, "Adaptive object slip prevention for prosthetic hands through proportional-derivative shear force feedback," in *2008 IEEE/RSJ International Conference on Intelligent Robots and Systems*. IEEE, 2008-09, pp. 1940,1945.
- [15] A. Tar and G. Cserey, "Development of a low cost 3d optical compliant tactile force sensor," in *2011 IEEE/ASME International Conference on Advanced Intelligent Mechatronics (AIM)*. IEEE, 2011-07, pp. 236,240.
- [16] L. S. Lincoln, M. Quigley, B. Rohrer, C. Salisbury, and J. Wheeler, "An optical 3d force sensor for biomedical devices," in *2012 4th IEEE RAS EMBS International Conference on Biomedical Robotics and Biomechanics (BioRob)*. IEEE, 2012-06, pp. 1500,1505.
- [17] H. Yousef, J.-P. Nikolovski, and E. Martincic, "Flexible 3d force tactile sensor for artificial skin for anthropomorphic robotic hand," *Procedia Engineering*, vol. 25, no. C, pp. 128,131, 2011.
- [18] N. Hale, M. Valero, J. Tang, D. Moser, and L. Jiang, "A preliminary study on characterisation of finger interface kinetics using a pressure and shear sensor system," *Prosthetics and Orthotics International*, vol. 42, no. 1, pp. 60,65, 2018-02.
- [19] A. Dwivedi, A. Ramakrishnan, A. Reddy, K. Patel, S. Ozel, and C. D. Onal, "Design, modeling, and validation of a soft magnetic 3-d force sensor," *IEEE Sensors Journal*, vol. 18, no. 9, pp. 3852,3863, 2018-05-01.
- [20] K. Nasir, R. L. A. Shauri, and J. Jaafar, "Calibration of embedded force sensor for robotic hand manipulation," in *2016 IEEE 12th International Colloquium on Signal Processing & Its Applications (CSPA)*. IEEE, 2016, pp. 351–355.
- [21] Y. Park, K. Chau, R. J. Black, and M. R. Cutkosky, "Force sensing robot fingers using embedded fiber bragg grating sensors and shape deposition manufacturing," in *Proceedings 2007 IEEE International Conference on Robotics and Automation*, April 2007, pp. 1510–1516.
- [22] A. Gomez Eguiluz, I. Rano, S. A. Coleman, and T. M. McGinnity, "Reliable object handover through tactile force sensing and effort control in the shadow robot hand," in *2017 IEEE International Conference on Robotics and Automation (ICRA)*. IEEE, 2017-05, pp. 372,377.
- [23] V. Ciobanu, D. Popescu, and A. Petrescu, "Point of contact location and normal force estimation using biomimetical tactile sensors," in *2014 Eighth International Conference on Complex, Intelligent and Software Intensive Systems*, July 2014, pp. 373–378.